Electronic Supplementary Material (ESI) for RSC Advances.

Supplementary Data

Study of Anisotropic Thermal conductivity in Textured Thermoelectric Alloys by Raman Spectra

Rapaka S C Bose, and K Ramesh*

Figure S1

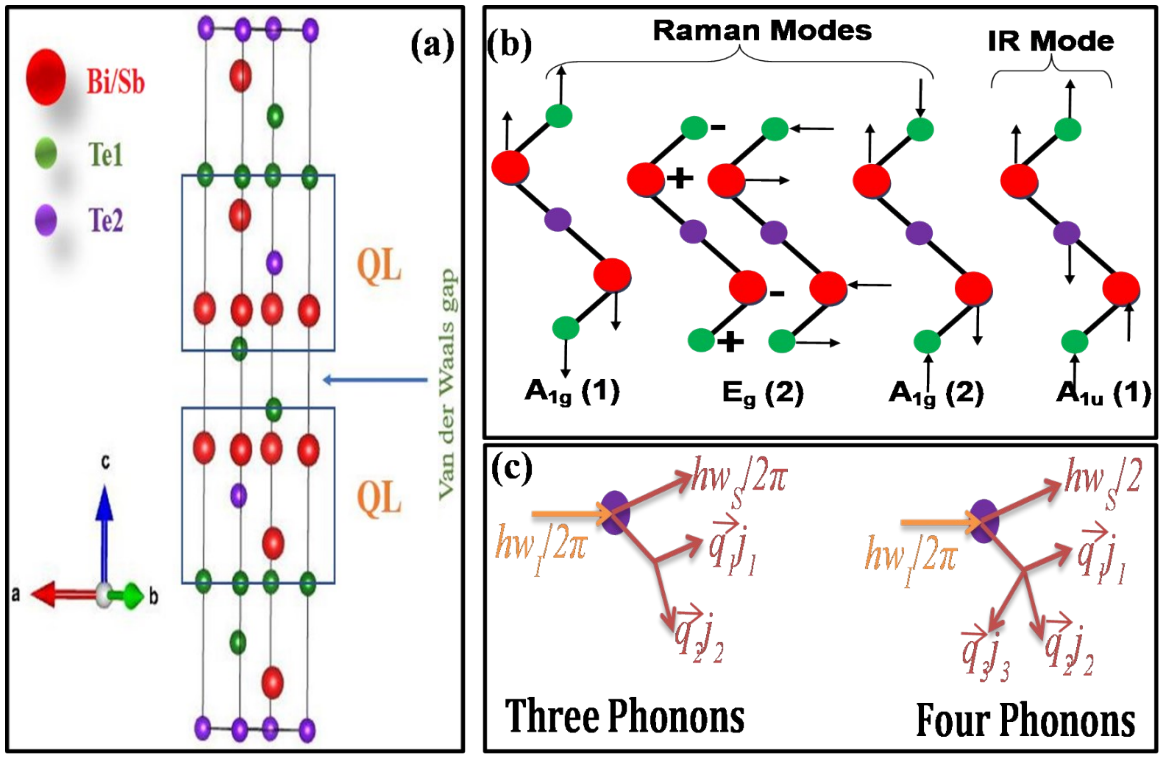

Fig. S1. (a) Crystal structure of Bi_2Te_3/Sb_2Te_3, **(b)** Schematic representation of Raman active modes, and **(c)** Schematic representation of the three-phonon and the four phonon decay processes.

Figure S2

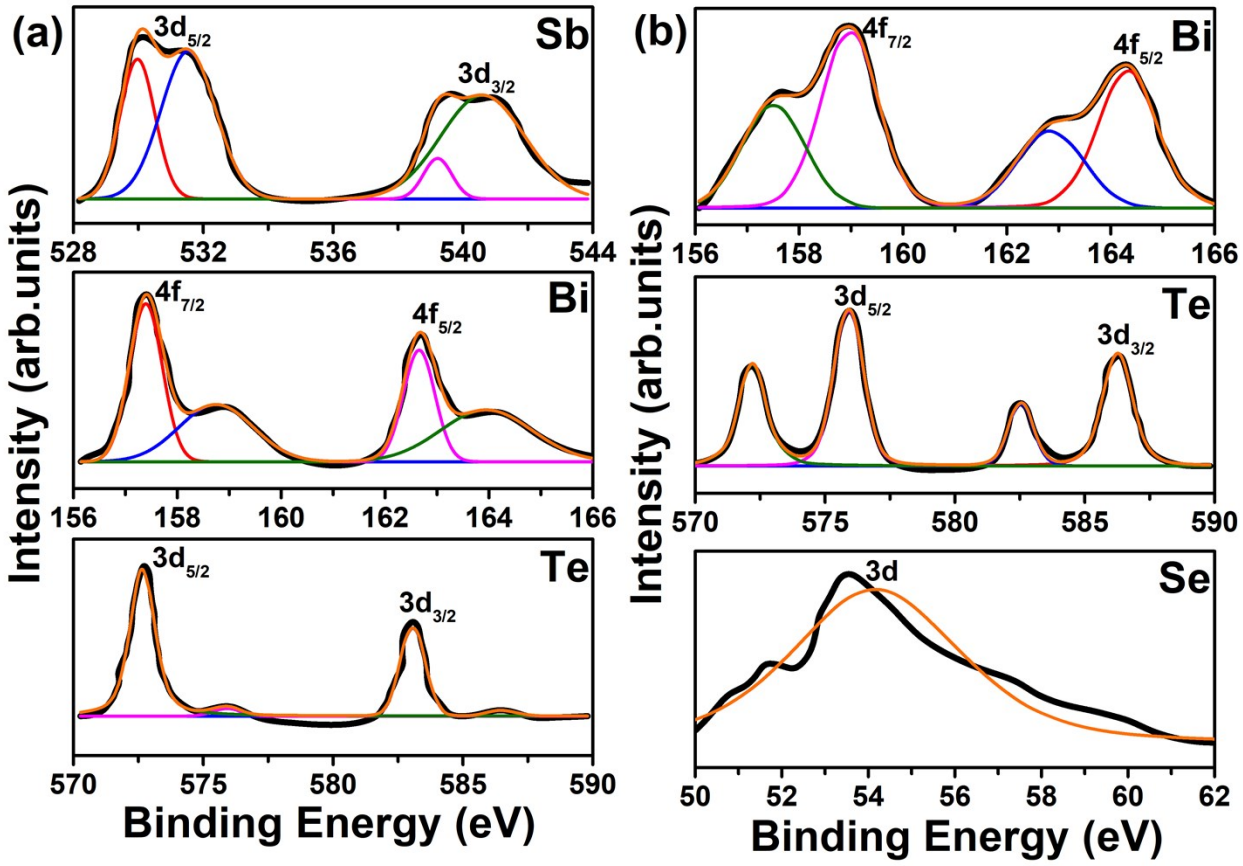

Fig. S2. XPS spectra of (a) *p*-type SBT (Sb 3*d*, Bi 4*f*, & Te 3*d*) and (b) *n*-type BTS (Bi 4*f*, Te 3*d*, & Se 3*d*).

Figure S3

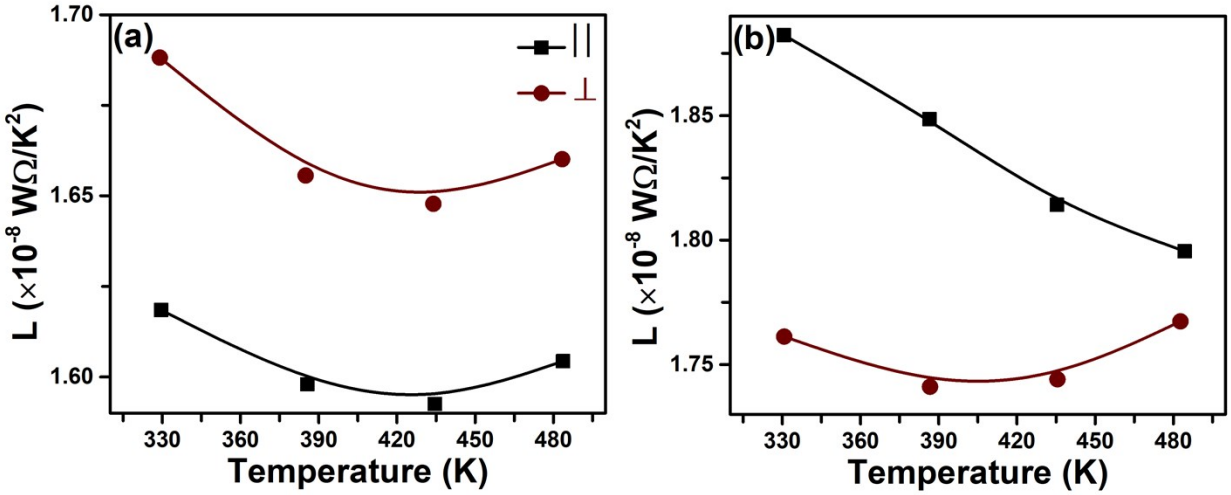

Fig. S3. Temperature dependent Lorenz number of **(a)** *p*-type SBT and **(b)** *n*-type BTS.

Figure S4

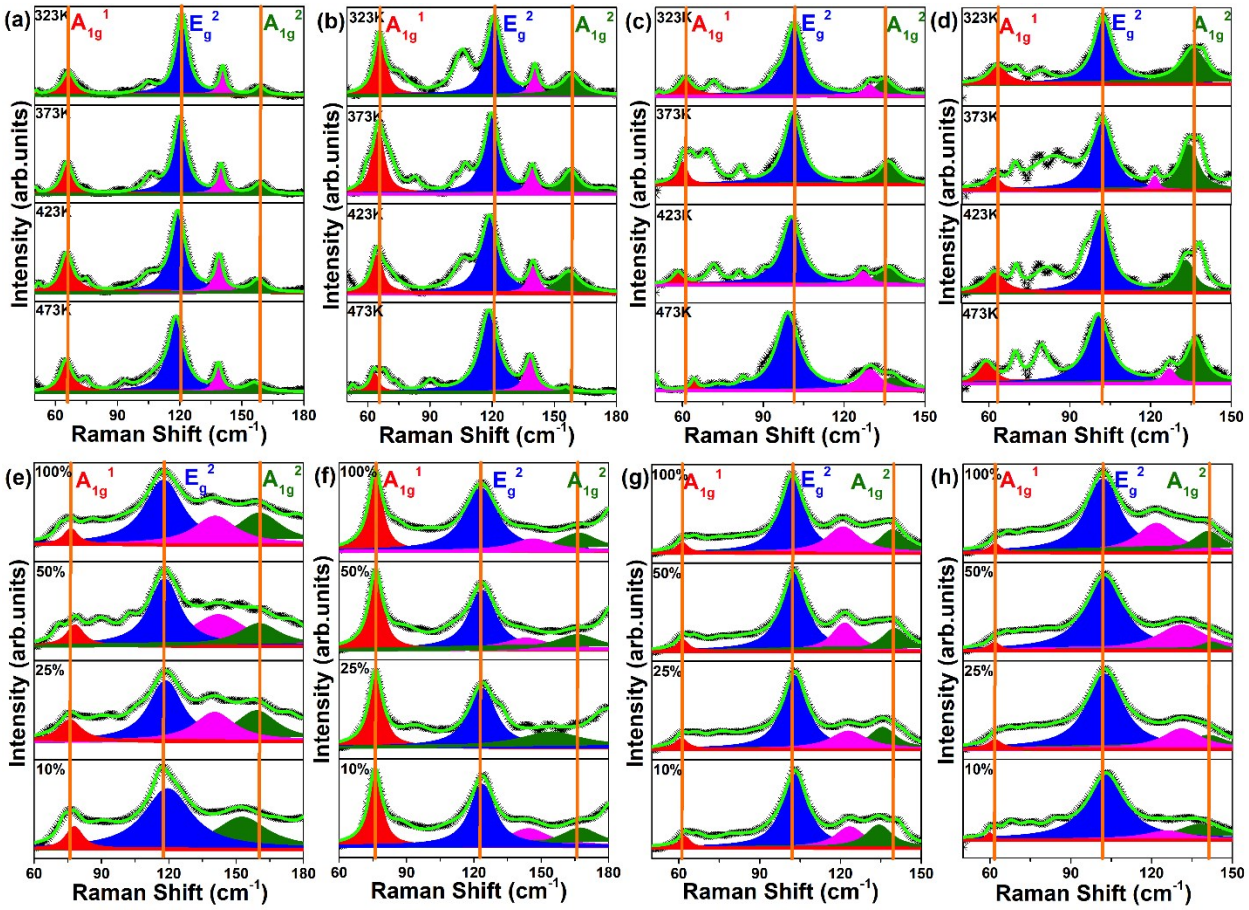

Fig. S4. Temperature dependent Raman spectra **(a)** Parallel direction, & **(b)** Perpendicular direction to the pressing axis; Laser power dependent **(c)** Parallel direction, & **(d)** Perpendicular direction to the pressing axis of *p*-type SBT; and Temperature dependent Raman spectra **(e)** Parallel direction, & **(f)** Perpendicular direction to the pressing axis; Laser power dependent **(g)** Parallel direction, & **(h)** Perpendicular direction to the pressing axis of *n*-type BTS.

Figure S5

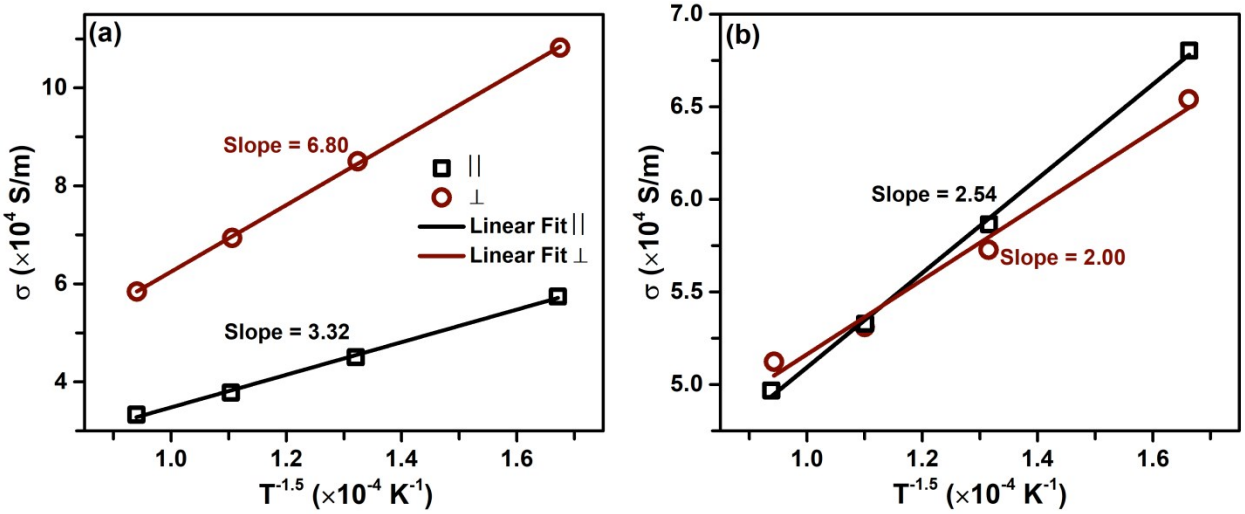

Fig. S5. Linear plot between σ and $T^{-1.5}$ of **(a)** *p*-type SBT and **(b)** *n*-type BTS.

Figure S6

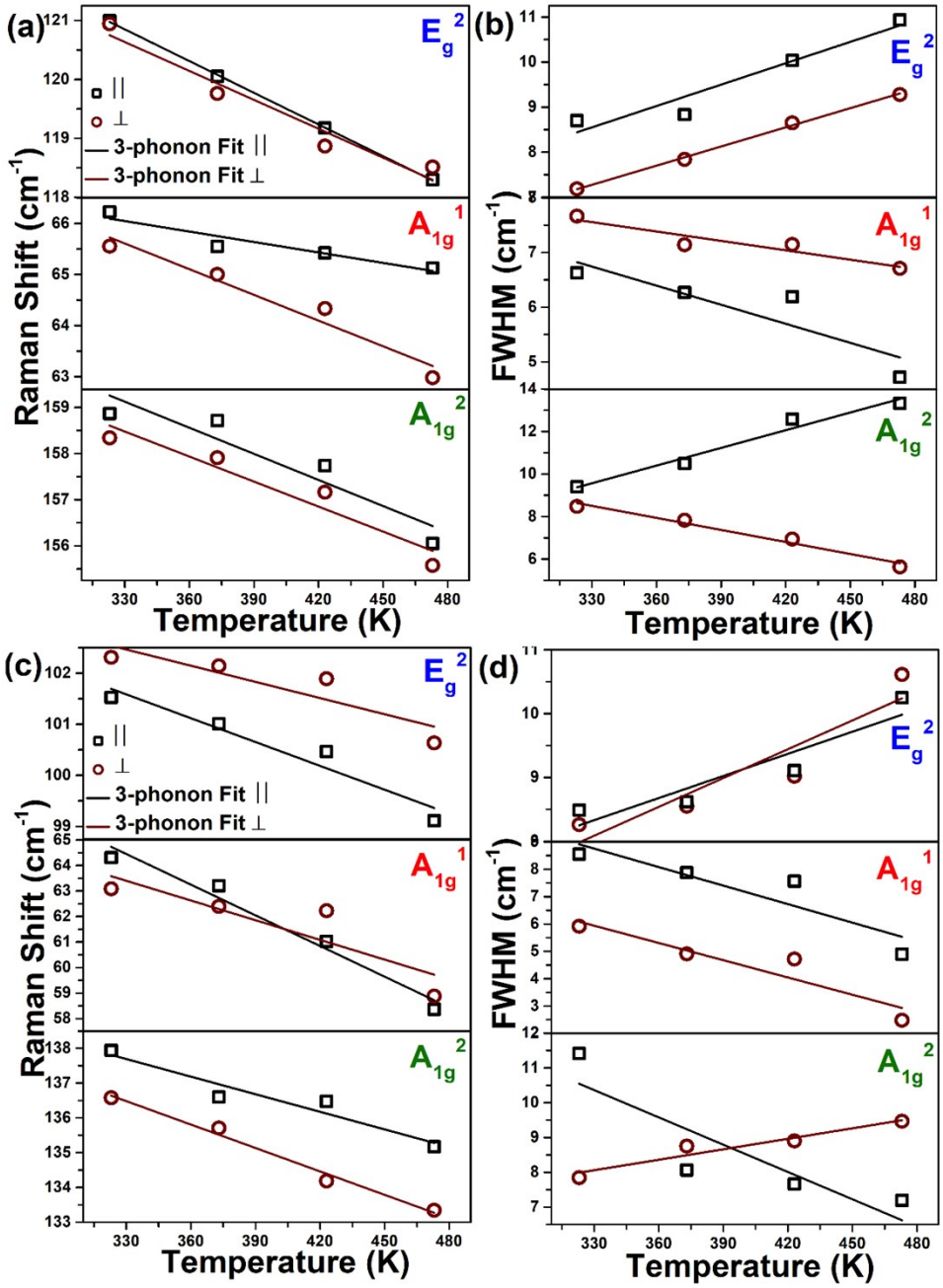

Fig. S6. Temperature dependent **(a)** Raman peak positions, & **(b)** FWHM of *p*-type SBT; and Temperature dependent **(c)** Raman peak positions, & **(d)** FWHM of *n*-type BTS.

Figure S7

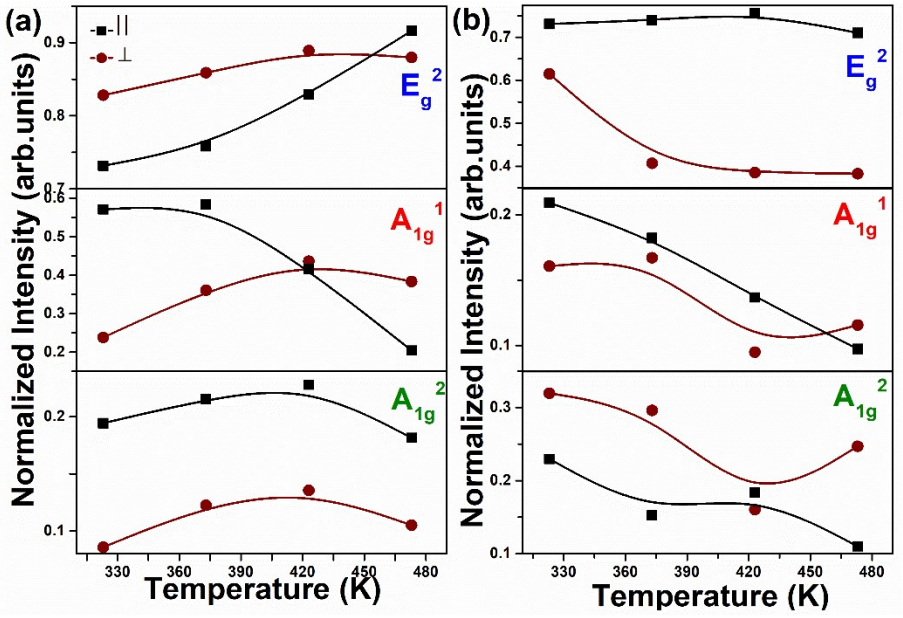

Fig. S7. Temperature dependent mode wise intensity of **(a)** *p*-type SBT, and **(b)** *n*-type BTS.

Table S1

Table S1. Raman active peaks of *p*-type SBT and *n*-type BTS in both directions: parallel and perpendicular to the pressing axis.

	***p*-type SBT**		***n*-type BTS**	
	Parallel (∥)	**Perpendicular (⊥)**	**Parallel (∥)**	**Perpendicular (⊥)**
E_g^2	~117. 69	~123.14	~102.05	~101.98
A_{1g}^1	~76.35	~76.07	~61.34	~61.92
A_{1g}^2	~160.33	~166.65	~139.33	~141.02